Dithiolene-like Platinum Complexes of the Methyl Esters of N^3-Isopropyl and t-Butyl Substituted Dithiocarbazic Acids. Crystal and Molecular Structures of $[\mathrm{Pt\{NPr^iNC(S)SMe\}_2}]$ and $[\mathrm{Pt\{NBu^tNC(S)SMe\}_2}]$†

Mario Bonamico, Vincenzo Fares, Patrizia Imperatori,* Lorenza Suber, and Franco Tarli*
Istituto di Teoria e Struttura Elettronica e Comportamento Spettrochimico dei Composti di Coordinazione del C.N.R., Area della Ricerca di Roma, C.P. n. 10, 00016 Monterotondo Stazione, Roma, Italy

The crystal and molecular structures of dithiolene-like $[\mathrm{Pt\{NPr^iNC(S)SMe\}_2}]$ and $[\mathrm{Pt\{NBu^tNC(S)SMe\}_2}]$ have been determined: both complexes have square-planar *trans*-$\mathrm{PtN_2S_2}$ chromophores. Their electronic and i.r. spectra have been recorded, and electrochemical investigations performed.

We have recently reported the results of an investigation on platinum complexes of some esters of dithiocarbazic acid and their N^3-substituted derivatives.[1–3] We have shown that the ligands co-ordinate through the terminal N and the thiono S atoms in neutral or in anionic deprotonated form and that the deeply coloured complexes containing the doubly deprotonated ligands are dithiolene-like and contain platinum in the +2 oxidation state.[8] Here we report a development of that work dealing with platinum complexes of the N^3 isopropyl and N^3 t-butyl derivatives of the methyl ester of dithiocarbazic acid containing the deprotonated ligands. Hereafter $\mathrm{NH_2NHC(S)SMe} = \mathrm{L}$, $\mathrm{NHPr^iNHC(S)SMe} = \mathrm{Pr^iL}$, and $\mathrm{NHBu^tNHC(S)SMe} = \mathrm{Bu^tL}$.

Experimental

Materials. The ligands $\mathrm{Pr^iL}$ and $\mathrm{Bu^tL}$ were prepared as reported in refs. 2 and 4, respectively.

Preparation of the Complexes.—The complex $[\mathrm{Pt(Pr^iL - H)_2}]$ $[\mathrm{Pr^iL - H} = \mathrm{NHPr^iN{=}C(S)SMe}]$ was prepared by adding a solution of $\mathrm{K_2[PtCl_4]}$ (0.98 mmol) in water (30 cm^3) to a stirred solution of $\mathrm{Pr^iL}$ (1.98 mmol) in EtOH (50 cm^3) in a nitrogen atmosphere. The solution was neutralized with 37% ammonia. After stirring for 5 h at room temperature the yellow product was filtered off, washed with water–ethanol (1:2) and dried (yield 50%) (Found: C, 22.90; H, 4.1; N, 10.4. Calc: C, 23.0; H, 4.25; N, 10.75%). The complex $[\mathrm{Pt(Bu^tL - H)_2}]$ $[\mathrm{Bu^tL - H} = \mathrm{NHBu^tN{=}C(S)SMe}]$ was prepared similarly. Yield 50% (Found: C, 26.00; H, 4.70, N, 10.10. Calc.: C, 26.2; H, 4.75; N, 10.2%). The complex $[\mathrm{Pt(Pr^iL - 2H)_2}]$ $[\mathrm{Pr^iL - 2H} = \mathrm{NPr^iNC(S)SMe}]$ was prepared as in ref. 2.

$[\mathrm{Pt(Bu^tL - 2H)_2}]$ $[\mathrm{Bu^tL - 2H} = \mathrm{NBu^tNC(S)SMe}]$. A solution of $\mathrm{K_2[PtCl_4]}$ (1.23 mmol) in water (20 cm^3) was added to a stirred solution of $\mathrm{Bu^tL}$ (2.47 mmol) in EtOH (50 cm^3) at room temperature. After 15 min, 37% ammonia was added to pH 9 and 30% aqueous $\mathrm{H_2O_2}$ (25 cm^3) was added dropwise. After stirring for 3 h the complex was filtered off, dried, and crystallized from boiling n-hexane. Yield 50%. Red-green dichroic crystals (Found: C, 26.55; H, 4.55; N, 9.95. Calc.: C, 26.3; H, 4.40; N, 10.25%).

Physical Measurements.—Microanalyses were performed by the Microanalytical Service of the Area della Ricerca di Roma del C.N.R. The visible–ultraviolet spectra and magnetic moments were measured as in ref. 1. Infra-red spectra were recorded with a Perkin-Elmer 983 spectrophotometer. D.c. polarography and cyclovoltammetry were performed as in ref. 5. All potentials reported are quoted with respect to the saturated calomel electrode (s.c.e.) with an accuracy of ±5 mV.

Table 1. Atomic co-ordinates with estimated standard deviations (e.s.d.s) in parentheses for $[\mathrm{Pt\{NPr^iNC(S)SMe\}_2}]$

Atom	x	y	z
Pt	0	0	0
S(1)	0.131 3(1)	0.282 7(2)	−0.053 79(4)
S(2)	−0.007 6(1)	0.629 6(2)	−0.185 84(4)
N(1)	−0.173 9(2)	0.129 4(5)	−0.077 2(1)
N(2)	−0.161 6(2)	0.308 4(5)	−0.127 5(1)
C(1)	−0.021 3(3)	0.391 4(6)	−0.121 0(2)
C(2)	0.193 9(3)	0.673 9(7)	−0.169 2(2)
C(3)	−0.336 1(3)	0.042 9(6)	−0.089 3(2)
C(4)	−0.394 6(4)	−0.059 8(8)	−0.168 5(3)
C(5)	−0.434 1(4)	0.258 5(9)	−0.073 2(3)

Table 2. Bond distances (Å) and angles (°), with e.s.d.s in parentheses for $[\mathrm{Pt\{NPr^iNC(S)SMe\}_2}]$

Pt–S(1)	2.274(1)	N(1)–N(2)	1.340(4)
Pt–N(2)	1.955(3)	N(1)–C(1)	1.317(4)
S(1)–C(1)	1.703(3)	N(2)–C(3)	1.497(4)
S(2)–C(1)	1.751(3)	C(3)–C(4)	1.510(6)
S(2)–C(2)	1.786(4)	C(3)–C(5)	1.516(6)
S(1)–Pt–N(2)	82.62(7)	S(1)–C(1)–S(2)	123.3(2)
Pt–S(1)–C(1)	96.7(1)	S(1)–C(1)–N(1)	122.8(2)
C(1)–S(2)–C(2)	102.6(2)	S(2)–C(1)–N(1)	113.9(2)
N(2)–N(1)–C(1)	114.4(3)	N(2)–C(3)–C(4)	110.5(3)
Pt–N(2)–N(1)	123.5(2)	N(2)–C(3)–C(5)	94.3(2)
Pt–N(2)–C(3)	125.6(2)	C(4)–C(3)–C(5)	111.8(4)
N(1)–N(2)–C(3)	110.9(2)		

Crystal Structure Determinations.—*Crystal data for* $[\mathrm{Pt\{NPr^iNC(S)SMe\}_2}]$. $\mathrm{C_{10}H_{20}N_4PtS_4}$, $M = 519.65$, monoclinic, $a = 9.027(1)$, $b = 5.285(1)$, $c = 18.217(3)$ Å, $\beta = 104.24(1)°$, $U = 842.4(3)$ Å^3, space group $P2_1/c$, $Z = 2$, $D_c = 2.049$ g cm^{-3}, dichroic red-green crystals, $\lambda(\text{Mo-}K_\alpha) = 0.710\,69$ Å, $\mu(\text{Mo-}K_\alpha) = 98.18$ cm^{-1}, $F(000) = 500$.

A selected crystal (0.1 × 0.1 × 0.4 mm) was used for data collection, at room temperature, on a Nicolet automated four-circle diffractometer by the θ—2θ scan technique with graphite-monochromated Mo-K_α radiation. 2 724 Reflections were collected ($3.5 \leqslant 2\theta \leqslant 60°$), 2 262 of which, having $I \geqslant 3\sigma(I)$, were used in the refinement. Data were corrected for Lorentz

---

† Bis[methyl 3-isopropyl- and bis[methyl 3-t-butyl-dithiocarbazato(2−)-N^3S]platinum(II).

Supplementary data available: see Instructions for Authors, *J. Chem. Soc., Dalton Trans.*, 1990, Issue 1, pp. xix—xxii.

Table 3. Atomic co-ordinates with e.s.d.s in parentheses for [Pt{N-$\mathrm{Bu^t}$NC(S)SMe}$_2$]

Atom	*x*	*y*	*z*
Pt	0	0	0
S(1)	0.096 4(2)	0.227 2(1)	−0.096 6(2)
S(2)	0.290 9(2)	0.276 3(2)	−0.339 0(2)
N(1)	0.188 5(5)	−0.004 3(4)	−0.248 6(4)
N(2)	0.111 6(5)	−0.092 9(4)	−0.155 6(4)
C(1)	0.188 4(6)	0.146 7(5)	−0.229 5(5)
C(2)	0.378(1)	0.148 8(7)	−0.455 5(7)
C(3)	0.128 3(7)	−0.262 4(4)	−0.188 2(5)
C(4)	0.237(1)	−0.276 3(6)	−0.310 9(7)
C(5)	−0.105 7(8)	−0.410 0(5)	−0.256 1(6)
C(6)	0.274 1(8)	−0.268 2(6)	−0.032 7(6)

Table 4. Bond distances (Å) and angles (°), with e.s.d.s in parentheses for [Pt{N$\mathrm{Bu^t}$NC(S)SMe}$_2$]

Pt–S(1)	2.278(1)	N(1)–C(1)	1.308(5)
Pt–N(2)	1.998(3)	N(2)–C(3)	1.521(5)
S(1)–C(1)	1.694(4)	C(3)–C(4)	1.534(7)
S(2)–C(1)	1.738(4)	C(3)–C(5)	1.53(1)
S(2)–C(2)	1.792(6)	C(3)–C(6)	1.533(8)
N(1)–N(2)	1.343(5)		
N(2)–Pt–S(1)	82.1(1)	S(2)–C(1)–N(1)	120.4(3)
Pt–S(1)–C(1)	97.5(2)	N(2)–C(3)–C(4)	110.8(4)
C(1)–S(2)–C(2)	102.5(3)	N(2)–C(3)–C(5)	108.3(4)
N(2)–N(1)–C(1)	116.0(3)	N(2)–C(3)–C(6)	108.7(5)
Pt–N(2)–C(3)	128.5(2)	C(4)–C(3)–C(5)	108.5(5)
N(1)–N(2)–C(3)	109.7(3)	C(4)–C(3)–C(6)	108.0(4)
S(1)–C(1)–S(2)	117.0(2)	C(5)–C(3)–C(6)	112.6(4)
S(1)–C(1)–N(1)	122.6(3)		

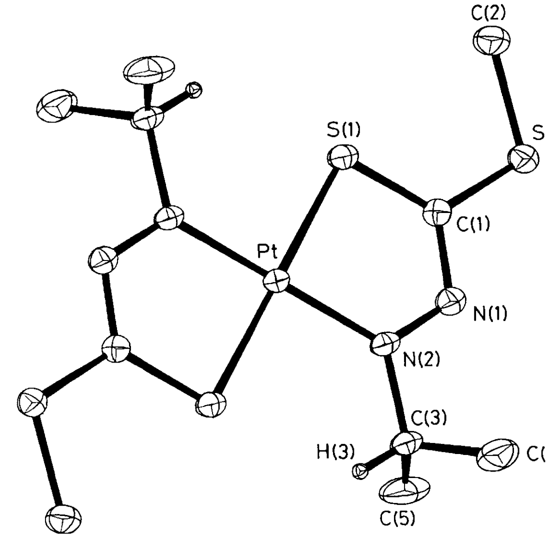

Figure 1. Perspective view of the molecular structure of the isopropyl derivative with the labelling scheme. Thermal ellipsoids are drawn at the 30% probability level

Table 5. I.r. data (cm^{-1}) for platinum complexes of $\mathrm{Pr^iL}$

$\mathrm{Pr^iL}$	[Pt($\mathrm{Pr^iL}$ − H)$_2$]	[Pt($\mathrm{Pr^iL}$ − 2H)$_2$]	Tentative assignment (prevalent contribution)
3 211m	3 049s		ν(N–H)
3 136m			
3 032m			
1 531s			δ(N–H) + ν(C $\overset{\cdots}{-}$ N)
	1 552s	1 464m	ν(C $\overset{\cdots}{-}$ N)
1 093w	997s	1 093s	ν(C–S) + ν(N–N)
1 076m	930s	1 070w	
1 036s		961w	
958s			
	524w	525w	ν(Pt–N)
	473w		
	371w	353w	ν(Pt–S)

Table 6. I.r. data (cm^{-1}) for platinum complexes of $\mathrm{Bu^tL}$

$\mathrm{Bu^tL}$	[Pt($\mathrm{Bu^tL}$ − H)$_2$]	[Pt($\mathrm{Bu^tL}$ − 2H)$_2$]	Tentative assignment (prevalent contribution)
3 220s	3 130m		ν(N–H)
3 148s	3 068m		
3 052m	3 036m		
1 534s			δ(N–H) + ν(C $\overset{\cdots}{-}$ N)
	1 532s	1 426m	ν(C $\overset{\cdots}{-}$ N)
	1 520 (sh)		
	1 510 (sh)		
1 084s	1 092w	1 068m	ν(C–S) + ν(N–N)
1 049s	1 006vs	1 027m	
1 026s	990vs	970w	
969s	960s	914vw	
	528w	525w	ν(Pt–N)
	353w	355w	ν(Pt–S)
	319w	320w	

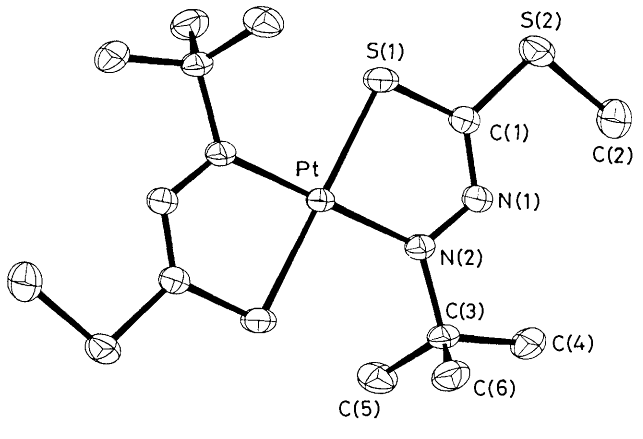

Figure 2. Molecular structure of the t-butyl derivative

polarization and a semiempirical absorption correction, based on a 360° scan around the scattering vector of selected reflections, was applied. The structure was solved by Patterson and Fourier methods and refined by the full-matrix least-squares method using anisotropic thermal parameters for all non-hydrogen atoms. The hydrogen atoms were located by a Fourier difference map and introduced in calculated positions with a fixed isotropic thermal parameter of 5.0 Å^2.

Final values for $R = \Sigma|\Delta F|/\Sigma|F_o|$ and $R' = [\Sigma w(\Delta F)^2/\Sigma w|F_o|^2]^{\frac{1}{2}}$ were 0.021 and 0.020 respectively, the weighting scheme being $w = 1/[\sigma(F_o)]^2$. Final atomic co-ordinates for non-hydrogen atoms are given in Table 1, interatomic distances and angles in Table 2. Neutral scattering factors (f' and f'') were used.[6] Computations were performed on an IBM 4361/4 computer using the SIR-CAOS crystallographic program system.[7]

Crystal data for [Pt{N$\mathrm{Bu^t}$NC(S)Me}$_2$]. $C_{12}H_{24}N_4PtS_4$, M = 547.70, triclinic, a = 7.005(1), b = 8.791(1), c = 9.183(2) Å, α = 100.21(2), β = 105.93(2), γ = 111.75(1)°, U = 479.8(2) Å^3, space group $P\bar{1}$, D_c = 1.896 g cm^{-3}, dichroic red-green prisms, Z = 1, λ(Mo-K_α) = 0.710 69 Å, μ(Mo-K_α) = 81.02 cm^{-1}, F(000) = 266.

A crystal 0.2 × 0.2 × 0.4 mm was selected. 2 802 Reflections were collected, 2 760 with $I \geqslant 3\sigma(I)$ being used in the refinement. Final values for R and R' were 0.027 and 0.028 respectively. Details of the procedure are given above. Final atomic co-ordinates for non-hydrogen atoms are given in Table 3, interatomic distances and angles in Table 4.

Additional material available from the Cambridge Crystallographic Data Centre comprises thermal parameters.

Results and Discussion

Preparation and Properties of the Platinum Complexes.—Both the ligands Pr^{i}L and Bu^{t}L react readily with $K_2[PtCl_4]$ in aqueous ethanol. We assume in solution a progressive deprotonation of the ligand: in the absence of oxidants and in an inert atmosphere the singly deprotonated yellow complexes [Pt(Pr^{i}L − H)$_2$] and [Pt(Bu^{t}L − H)$_2$] are formed whereas in air they turn into the deep coloured doubly deprotonated complexes [Pt(Pr^{i}L − 2H)$_2$] and [Pt(Bu^{t}L − 2H)$_2$].

Table 7. Solution electronic spectra (10^3 cm^{-1}) of the platinum complexes with doubly deprotonated ligands[a]

Compound	Chromophore	
[Pt(Pr^{i}L − 2H)$_2$]	*trans*-PtN$_2$S$_2$[b]	14.5 (4.44), 20.9(sh) (3.14), 22.8 (3.28), 28.1 (3.32), 32.0(sh) (3.54), 35.9(sh) (4.05), 38.6 (4.20)
[Pt(Bu^{t}L − 2H)$_2$]	*trans*-PtN$_2$S$_2$[b]	13.3 (4.33), 20.4(sh) (3.12), 21.7 (3.15), 26.8(sh) (3.34), 30.8(sh) (3.59), 34.8(sh) (3.93), 38.6 (4.26)
[Pt(PhL − 2H)$_2$]	*trans*-PtN$_2$S$_2$[c]	13.5 (4.43), 21.8(sh) (3.76), 23.9 (3.85), 31.2 (4.18), 39.0(sh) (4.23)
[Pt(L − 2H)$_2$]	*trans*-PtN$_2$S$_2$[d]	15.0 (4.50), 22.4 (3.20), 27.4 (3.26), 37.9 (4.23)

[a] log(ε/dm^3 mol^{-1} cm^{-1}) in parentheses. In CH$_2$Cl$_2$. [b] See text. [c] See ref. 10. [d] See ref. 1.

Description of the Structures.—The molecular structures of the isopropyl and t-butyl derivatives are shown in Figures 1 and 2 respectively. In both compounds the Pt atom lies on a centre of symmetry in a distorted square planar arrangement. The C(3)N(2)N(1)C(1)S(1)S(2)C(2) ligand system is highly planar, in a *cis-cis* conformation for the isopropyl derivative and *cis-trans* for the t-butyl one. The crystal packing consists of monomeric units; no intermolecular interactions below 3.6 Å are present between symmetry-related molecules in both compounds. There are just a few weak intramolecular contacts among the methyl groups and S(1) or N(1) [C(2) ··· S(1) 3.10 Å for the isopropyl and C(2) ··· N(1) 2.86 Å for the t-butyl derivative]; these weak interactions however are not sufficient to justify the different conformations that, probably of similar energy, are determined only by the crystallization process. The accuracy of the bond distances and angles is better than that obtained for the previously studied compounds: the values substantially confirm those found for the benzyl and the phenyl derivatives[2,8], with the exception of Pt–N(2) and N(2)–C(3) bonds. The progressive lengthening of the Pt–N(2) bond within the sequence benzyl, isopropyl, phenyl, and t-butyl derivatives [1.937(4), 1.955(3), 1.966(4), and 1.998(3) Å respectively] is in agreement with the electron-withdrawing effect of the sub-

Table 8. Electrochemical data for the oxidation of platinum complexes in CH$_2$Cl$_2$ solution (1 × 10^{-3} mol dm^{-3})[a]

	Cyclic voltammetry[b]					
Compound	E^1_p(an)/V	E^2_p(an)/V	ΔE^1_p[c]/V	ΔE^2_p[c]/V	i^1(an)/i^1(cat)	i^2(an)/i^2(cat)
[Pt(Pr^{i}L − 2H)$_2$]		1.045		0.100		0.88
[Pt(Bu^{t}L − 2H)$_2$]	1.310	0.920	0.120	0.100	*d*	1.60
[Pt(PhL − 2H)$_2$]		1.160		0.095		0.88

	D.c. voltammetry at a pulsing platinum electrode[e]					
	$E^1_{\frac{1}{2}}$/V	$E^2_{\frac{1}{2}}$/V	i^1/μA	i^2/μA	Slope^{1f}/V	Slope^{2f}/V
[Pt(Pr^{i}L − 2H)$_2$]		1.050		1.60		0.065
[Pt(Bu^{t}L − 2H)$_2$]	1.270	0.890	1.80	1.52	0.060	0.050
[Pt(PhL − 2H)$_2$]		1.110		1.56		0.080

[a] Containing 0.1 mol dm^{-3} NBu$_4$BF$_4$, 20 °C. [b] Scan rate 200 mV s^{-1}. [c] Anodic to cathodic peak potential separation. [d] Poorly resolved reduction wave. [e] Pulsing time t_p = 2s. [f] Calculated using $E_{\frac{3}{4}} - E_{\frac{1}{4}}$

Table 9. Electrochemical data for the reduction of platinum complexes in CH$_2$Cl$_2$ solution (1 × 10^{-3} mol dm^{-3})[a]

	Cyclic voltammetry[b]					
Compound	E^3_p(cat)/V	E^4_p(cat)/V	ΔE^3_p[c]/V	ΔE^4_p[c]/V	i^3(cat)/i^3(an)	i^4(cat)/i^4(an)
[Pt(Pr^{i}L − 2H)$_2$]	−0.560	−1.390	0.100	*d*	1.00	*d*
[Pt(Bu^{t}L − 2H)$_2$]	−0.565	−1.330	0.100	*d*	1.03	*d*
[Pt(PhL − 2H)$_2$]	−0.290	−0.910	0.100	0.100	1.10	1.48
[Pt(L − 2H)$_2$]	−0.320	−1.120	0.090	*d*	1.08	*d*

	D.c. voltammetry at a pulsing platinum electrode[e]					
	$E^3_{\frac{1}{2}}$/V	$E^4_{\frac{1}{2}}$/V	i^3/μA	i^4/μA	Slope^{3f}/V	Slope^{4f}/V
[Pt(Pr^{i}L − 2H)$_2$]	−0.550	−1.340	1.66	1.65	0.070	0.070
[Pt(Bu^{t}L − 2H)$_2$]	−0.530	−1.280	1.88	1.80	0.065	0.050
[Pt(PhL − 2H)$_2$]	−0.290	−0.890	1.12	1.26	0.070	0.070
[Pt(L − 2H)$_2$]	−0.300		0.36		0.060	

[a] Containing 0.1 mol dm^{-3} NBu$_4$BF$_4$, 20 °C. [b] Scan rate 200 mV s^{-1}. [c] Cathodic to anodic peak potential separation. [d] Poorly resolved oxidation wave. [e] Pulsing time t_p = 2s. [f] Calculated using $E_{\frac{3}{4}} - E_{\frac{1}{4}}$

stituents on N^3 and with the electronic spectra in solution (see below and ref. 2). The lengthening of the N(2)–C(3) bond, 1.429(7), 1.474(7), 1.497(4), and 1.521(5) Å respectively, for the phenyl, benzyl, isopropyl and t-butyl derivatives, can be related to the increase in the steric hindrance of the substituents on C(3), that prevails on the electronic effect.

Infra-red Spectra.—Infra-red spectral data are reported in Tables 5 and 6. The spectra of $[\mathrm{Pt(Pr^iL - H)_2}]$ and $[\mathrm{Pt(Bu^tL - H)_2}]$ show ν(N–H) bands shifted to lower frequencies with respect to the corresponding bands of the free ligands owing to N^3 co-ordination, and $\nu(\mathrm{C} \overset{\cdots}{-} \mathrm{N})$ of the partial double bonds of the singly deprotonated ligands at 1 552 and 1 532 $\mathrm{cm^{-1}}$, respectively. The spectra of $[\mathrm{Pt(Pr^iL - 2H)_2}]$ and $[\mathrm{Pt(Bu^tL - 2H)_2}]$ containing the doubly deprotonated ligands lack bands attributable to ν(N–H). New bands attributable to ν(Pt–S) and to ν(Pt–N) are found in the spectra of all the complexes owing to N,S chelation of the ligands. Bands attributable to $\nu(\mathrm{C} \overset{\cdots}{-} \mathrm{N})$ of the partial double bond are shifted to lower frequencies in the complexes containing the doubly deprotonated ligands because of the higher electronic delocalization over the whole molecule compared with the complexes containing the singly deprotonated ligands.

Electronic Spectra.—The electronic spectra of $[\mathrm{Pt(Pr^iL - 2H)_2}]$ and of $[\mathrm{Pt(Bu^tL - 2H)_2}]$ (Table 7) show features which are characteristic of dithiolene-like platinum complexes of dithiocarbazic esters,[1,2] with very intense charge transfer (c.t.) bands in the visible region. The shift of the bands follows the electron-withdrawing effect of substituents on N^3, $\mathrm{H} < \mathrm{Pr^i} < \mathrm{Ph} \leqslant \mathrm{Bu^t}$, in agreement with the effects observed on the basicity constants of alkyl- and aryl-substituted hydrazines which are lower than for unsubstituted ones.[2,9] We note the red shift of the c.t. band in the spectrum of $[\mathrm{Pt(Bu^tL - 2H)_2}]$ with respect to the spectrum of $[\mathrm{Pt(Pr^iL - 2H)_2}]$ which is attributable to the higher steric effect of $\mathrm{Bu^t}$.

Electrochemical Measurements.—The electrochemical behaviour of $[\mathrm{Pt(Pr^iL - 2H)_2}]$ and $[\mathrm{Pt(Bu^tL - 2H)_2}]$ in $\mathrm{CH_2Cl_2}$ solution shows the electron-transfer properties of both complexes as we reported previously for other platinum and nickel complexes with doubly deprotonated esters of dithiocarbazic acid.[1,2,10] They have been investigated by means of d.c. and cyclic voltammetry: data are reported in Tables 8 and 9. The voltage range 0 to +1.5 V was explored in oxidation and the range 0 to −1.5 V in reduction. All complexes show well defined polarographic waves corresponding to the formation of some species belonging to the Scheme. We note the formation of positive radicals which is unusual for dithiolene-like complexes with N,S-chelating ligands. The low reversibility of the radicals (**1**) and (**4**) indicates a moderate stability of these species in $\mathrm{CH_2Cl_2}$. In dimethylformamide stable radicals (**3**) and (**4**) were observed, but positive radicals (**1**) and (**2**) were not.[1,2]

$$\underset{(\mathbf{1})}{[\mathrm{Pt(NS)_2}]^{2+}} \underset{-\mathrm{le}}{\overset{+\mathrm{le}}{\rightleftarrows}} \underset{(\mathbf{2})}{[\mathrm{Pt(NS)_2}]^{+}} \underset{-\mathrm{le}}{\overset{+\mathrm{le}}{\rightleftarrows}} [\mathrm{Pt(NS)_2}] \underset{-\mathrm{le}}{\overset{+\mathrm{le}}{\rightleftarrows}} \underset{(\mathbf{3})}{[\mathrm{Pt(NS)_2}]^{-}} \underset{+\mathrm{le}}{\overset{+\mathrm{le}}{\rightleftarrows}} \underset{(\mathbf{4})}{[\mathrm{Pt(NS)_2}]^{2-}}$$

Scheme.

Acknowledgements

We thank G. Chiozzini, F. Dianetti, L. Petrilli, and C. Riccucci for the help in the experimental work and C. Veroli for drawings.

References

1 C. Battistoni, A. M. Giuliani, E. Paparazzo, and F. Tarli, *J. Chem. Soc., Dalton Trans.*, 1984, 1293.
2 V. Fares, A. M. Giuliani, P. Imperatori, L. Suber, and F. Tarli, *J. Chem. Soc., Dalton Trans.*, 1987, 1035.
3 A. M. Giuliani and F. Tarli, Proceedings of the 3rd International Conference on the Chemistry of the Platinum Group Metals, Sheffield, 1987, p. j–18.
4 K. A. Jensen, K. Anthoni, and A. Holm, *Acta Chem. Scand.*, 1969, **23**, 1916.
5 R. Andruzzi and A. Trazza, *J. Electroanal. Chem.*, 1978, **86**, 201.
6 'International Tables for *X*-Ray Crystallography,' Kynoch Press, Birmingham, 1974, vol. 4.
7 M. Camalli, D. Capitani, G. Cascarano, S. Cerrini, C. Giacovazzo, and R. Spagna SIR-CAOS, Ital. P. 35 403c/1986.
8 G. Dessy and V. Fares, *Acta Crystallogr., Sect. B*, 1980, **36**, 2266.
9 Houben-Weyl, 'Methoden in der organischen Chemie,' Georg Thieme, Stuttgart, 1967, vol. 10/2, p. 5.
10 D. Attanasio, V. Fares, P. Imperatori, G. Mattogno, and F. Tarli, *J. Chem. Soc., Dalton Trans.*, 1988, 1217.

Received 9*th May* 1989; *Paper* 9/01939A